The Astrophysical Journal, 726:32 (5pp), 2011 January 1 doi:10.1088/0004-637X/726/1/32

XRF 100316D/SN 2010bh: CLUE TO THE DIVERSE ORIGIN OF NEARBY SUPERNOVA-ASSOCIATED GAMMA-RAY BURSTS

Yi-Zhong Fan[1,2], Bib-Bin Zhang[2], Dong Xu[3], En-Wei Liang[2,4], and Bing Zhang[2]
[1] Purple Mountain Observatory, Chinese Academy of Science, Nanjing, 210008, China; yzfan@pmo.ac.cn
[2] Department of Physics and Astronomy, University of Nevada Las Vegas, Las Vegas, NV 89154, USA; zhang@physics.unlv.edu
[3] Benoziyo Center for Astrophysics, Faculty of Physics, The Weizmann Institute of Science, Rehovot 76100, Israel
[4] Department of Physics, Guangxi University, Guangxi 530004, China
Received 2010 April 24; accepted 2010 October 28; published 2010 December 13

ABSTRACT

X-ray Flash (XRF) 100316D, a nearby super-long underluminous burst with a peak energy $E_p \sim 20$ keV, was detected by *Swift* and was found to be associated with an energetic supernova SN 2010bh. Both the spectral and the temporal behavior are rather similar to XRF 060218, except that the latter was associated with a "less energetic" SN 2006aj and had a prominent soft thermal emission component in the spectrum. We analyze the spectral and temporal properties of this burst and interpret the prompt gamma-ray emission and the early X-ray plateau emission as synchrotron emission from a dissipating Poynting flux dominated outflow, probably powered by a magnetar with a spin period of $P \sim 10$ ms and the polar cap magnetic field $B_p \sim 3 \times 10^{15}$ G. The energetic supernova SN 2010bh associated with this burst is, however, difficult to interpret within the slow magnetar model, and we suspect that the nascent magnetar may spin much faster with an initial rotation period $\sim$1 ms. It suggests a delay between the core collapse and the emergence of the relativistic magnetar wind from the star. The diverse behaviors of low-luminosity gamma-ray bursts and their associated supernovae may be understood within a unified picture that invokes different initial powers of the central engine and different delay times between the core collapse and the emergence of the relativistic jet from the star.

Key words: gamma rays: general – radiation mechanisms: non-thermal – X-rays: general

Online-only material: color figures

1. INTRODUCTION

After four years of waiting since the detection of X-Ray Flash (XRF) 060218/SN 2006aj, another low-luminosity (LL) gamma-ray burst (GRB)–supernova (SN) pair association, XRF 100316D/SN 2010bh at redshift $z = 0.059$ (Vergani et al. 2010), was captured by *Swift* (Gehrels et al. 2004) on 2010 March 16 (Stamatikos et al. 2010; Wiersema et al. 2010; Chornock et al. 2010; Rau et al. 2010), with a detection rate fully consistent with the population studies of these nearby LL-GRB events (Coward 2005; Soderberg et al. 2006; Liang et al. 2007a; Guetta & Della Valle 2007). Before this event, four pairs of nearby ($z < 0.2$) secure GRB(XRF)–SN associations had been identified. These are GRB 980425/SN 1998bw at $z = 0.0085$ (e.g., Galama et al. 1998), GRB 030329/SN 2003dh at $z = 0.168$ (e.g., Hjorth et al. 2003), GRB 031203/SN 2003lw at $z = 0.105$ (e.g., Malesani et al. 2004), and XRF 060218/SN 2006aj at $z = 0.0331$ (e.g., Campana et al. 2006). The nature of the GRB/SN connection and the interplay between the GRB and the SN components are still poorly understood. In this paper, we analyze and interpret the *Swift* Burst Alert Telescope (BAT) and X-ray Telescope (XRT) data of XRF 100316D, paying special attention to the similarities and differences between the XRF 100316D/SN 2010bh and XRF 060218/SN 2006aj.

2. THE γ-RAY AND X-RAY OBSERVATIONS

GRB 100316D triggered *Swift*/BAT at 12:44:50 UT ($T_{\rm trig}$), and the XRT began observing the field 137.7 s after the BAT trigger (Stamatikos et al. 2010). A bright, steady uncataloged X-ray source was detected. By analyzing the BAT survey data before and after the trigger time, it is found that this event possibly started at $\sim(T_{\rm trig} - 1500)$ s (Stamatikos et al. 2010). However, the gamma-ray flux of the source kept almost constant from $T_{\rm trig} - 1500$ to $T_{\rm trig} - 500$ before increasing significantly at $T_{\rm trig} - 500$. We therefore take the starting time of this event as $T_{\rm trig} - 500$ s. The host galaxy redshift is $z = 0.059$ (Vergani et al. 2010). An associated supernova, SN 2010bh, was detected by Wiersema et al. (2010) and spectroscopically confirmed by Chornock et al. (2010).

We extract the observed light curves and spectra of XRF 100316D from the BAT and XRT event data. The details of our data reduction are presented in Zhang et al. (2007) and Liang et al. (2007b). The joint BAT/XRT spectrum from $T_{\rm trig} + 138$ s to $T_{\rm trig} + 736$ s is well fit with a cutoff power-law model, with a power-law index of 1.32 ± 0.03 and a spectral peak energy E_p of $19.6^{+3.3}_{-2.8}$ keV (χ^2/dof = 1320/1057, Figure 1).[5] This suggests that the X-ray and the gamma-ray emissions are from the same emission component. A time-resolved spectral analysis during the period from $T_{\rm trig} + 138$ s to $T_{\rm trig} + 736$ s shows that E_p clearly evolves with time, from $32.6^{+14.2}_{-8.5}$ keV (from $T_{\rm trig} + 138$ s to $T_{\rm trig} + 240$ s) to $18.3^{+3.9}_{-3.2}$ keV (from $T_{\rm trig} + 240$ s to $T_{\rm trig} + 734$ s). The unabsorbed light curves and the temporal evolution of E_p are shown in Figure 2, along with the data of GRB 060218. The late X-ray light curves of the other nearby GRBs, including GRB 980425, 031203, and 030929, are also displayed in Figure 2. The X-ray light curves of XRF 100316D and XRF 060218 are rather similar. Both have an plateau phase extending to more than 1000 s. In the case of XRF 100316D, there is an observational gap between $T_{\rm trig} + 736$ s and $T_{\rm trig} + 36437$ s. The late-time observational data (after $T_{\rm trig} + 36437$ s) are soft and

[5] The time-integrated BAT spectrum can be reasonably fitted by a single power $F_\nu \propto \nu^{-2.5\pm0.3}$. Together with the joint BAT–XRT fit, we are able to constrain $E_p \sim 20$ keV and therefore define this burst as an XRF.

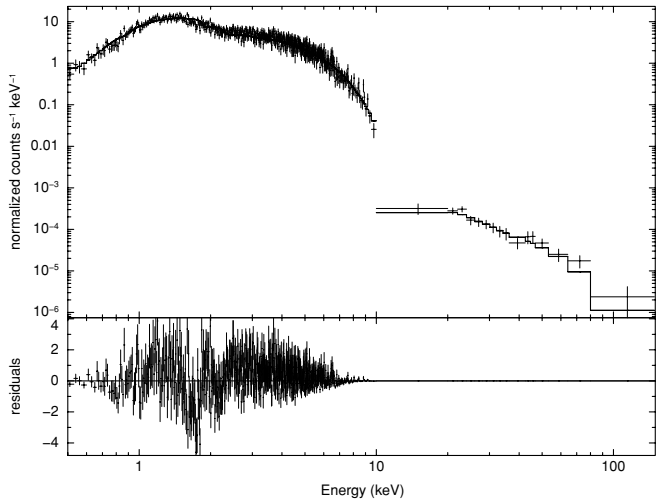

Figure 1. Joint BAT+XRT spectrum of XRF 100316D with a cutoff power-law model fit (line) for the time-integrated spectrum from $T_{\rm trig}$ + 138 s to $T_{\rm trig}$ + 736 s. The model parameters are $\Gamma = 1.32 \pm 0.03$ and $E_{\rm p} = 19.6^{+3.3}_{-2.8}$ keV.

consistent with a single power-law decay with a decay index $\alpha = 1.31 \pm 0.21$. This is similar to the late X-ray light curve of XRF 060218. XRF 060218 also shows a steep decay phase between the plateau and the late single power-law decay phase. Although this is not observed in XRF 100316D, the data before $T_{\rm trig}$ + 734 s and after $T_{\rm trig}$ + 36437 s are consistent with having such a steep decay segment in between.

There are however some differences between the two events. First, the X-ray data of XRF 060218 demand a soft thermal emission component with an evolving temperature, which has been interpreted as due to shock breakout from the progenitor star (Campana et al. 2006). For XRF 100316D, we find that the data do not demand such a component. We noticed that Starling et al. (2010) claimed a thermal component with $kT \sim 0.14$ keV and an energy that is ∼3% of the entire X-ray emission. To check the consistency, we fit the time-dependent BAT+XRT joint spectra by a cutoff power-law model (with absorption from both Milk Way and the host galaxy, wabs*zwabs*cutoffpl in Xspec 12) and a blackbody+cutoff power-law model. We find that both models can give equally acceptable fits to the data. For example, for the slice 2 (from $T_{\rm trig}$ + 240 s to $T_{\rm trig}$ + 734 s), the former model gives $\chi^2/{\rm dof} = 1305/1085$ with $N_{\rm gal} = 7.05 \times 10^{20}$ cm^{-2} and $N_{\rm H,host} = 4.6 \times 10^{21}$ cm^{-2}, while the latter gives $\chi^2/{\rm dof} = 1264/1085$ with a larger host galaxy absorption $N_{\rm H,host} = 1.3 \times 10^{22}$ cm^{-2} and a thermal temperature that is consistent with Starling et al. (2010). Note that the peak of the proposed blackbody component is near the low end of the XRT energy band and the neutral hydrogen absorption around the thermal peak is large. This results in great uncertainty in identification of such a thermal emission component from the data. Our spectral analysis cannot robustly identify this component, although χ^2 is slightly improved by adding it. Therefore, we do not claim a thermal emission in the observed spectrum and only stick to the cutoff power-law model to discuss possible theoretical implications. The second difference between the two events lies in the supernova data. The modeling of SN 2006aj suggests a kinetic energy $\sim 2.5 \times 10^{51}$ erg (Mazzali et al. 2006b), much smaller than that of other supernovae (SNe) associated with nearby GRBs (see Figure 3). Although the modeling of SN 2010bh is not available yet, current data imply an SN event as energetic as SN 1998bw

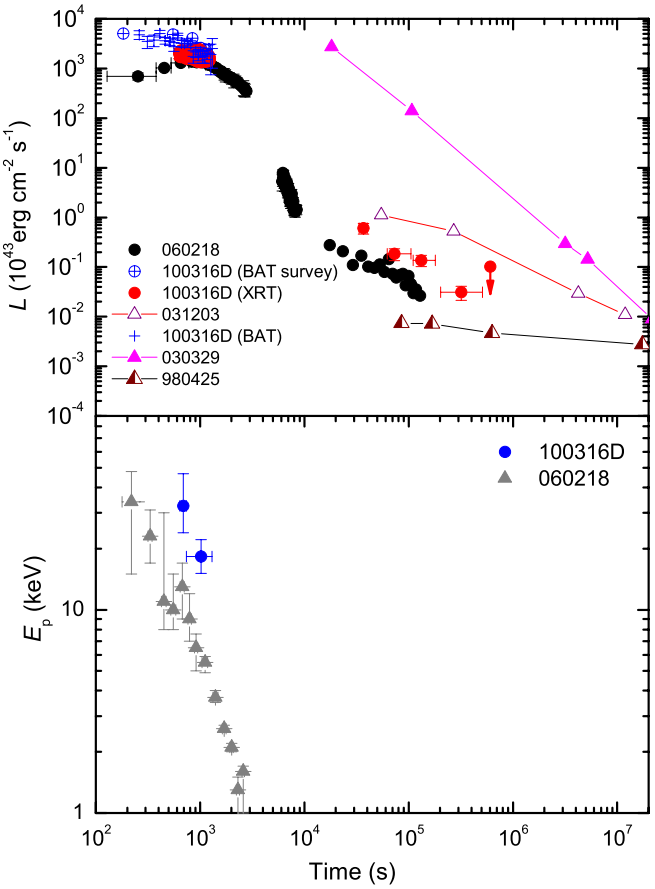

Figure 2. Upper: unabsorbed luminosity light curve in the XRT band of GRB 100316D in comparison with GRBs 980425, 030329, 031203, and 060128. The BAT data of GRB 100316D are extrapolated to the XRT band. Lower: comparison of the $E_{\rm p}$ temporal evolution of GRB0100316D with GRB 060218. The $E_{\rm p}$ data of GRB 060218 are taken from Toma et al. (2007).

(A color version of this figure is available in the online journal.)

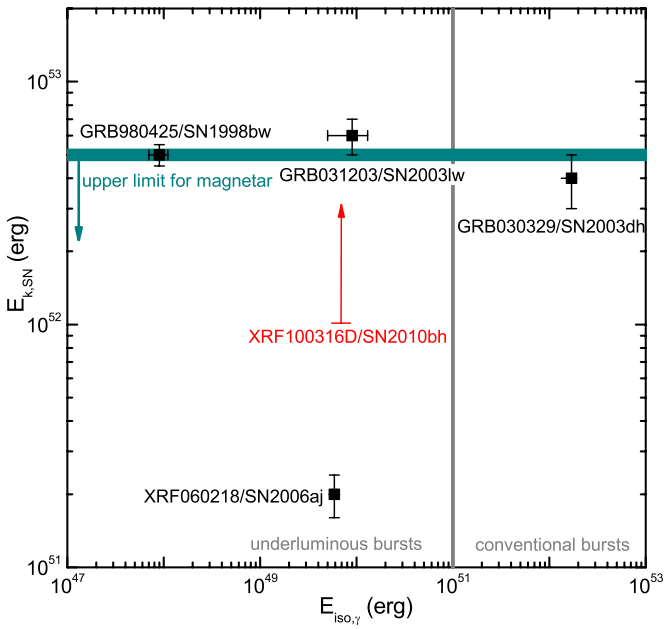

Figure 3. Isotropic energy of the prompt emission vs. the kinetic energy of the supernova outflow. The kinetic energy of SN 2010bh is estimated to be larger than $\sim 10^{52}$ erg (see footnote 6). Other data are taken from Li (2006). The possible maximum energy $\sim 5 \times 10^{52}$ erg that can be provided by a pulsar with $P \lesssim 1$ ms and $I \sim 2 \times 10^{45}$ g cm^2 is also plotted.

(A color version of this figure is available in the online journal.)

(Chornock et al. 2010),[6] which is about one order of magnitude more energetic than SN 2006aj. So from the observational point of view, XRF 100316D/SN 2010bh and XRF 060218/SN 2006aj are not strictly "twins."

3. A POSSIBLE MODEL FOR THE LONG-LASTING X-RAY PLATEAU

In the following, we define $t = T - T_{\rm trig} + 500$ s, i.e., the time elapse since $T_{\rm trig} - 500$ s. We interpret all the BAT/XRT data of XRF 100316D for $0 \leqslant t \leqslant 1.23 \times 10^3$ s as "prompt emission" (i.e., the radiation powered by some internal energy dissipation processes) for the following two reasons. First, the steady plateau behavior observed in both BAT and XRT band at $t \leqslant 1.23 \times 10^3$ s with an evolving E_p is difficult to interpret within afterglow models. Second, the sharp decline of the X-ray emission (t^{-2} or even steeper) expected in the time interval 1.23×10^3 s $< t < 3 \times 10^4$ s resembles the early rapid decline that has been detected in a considerable fraction of *Swift* GRBs, which is widely taken as a piece of evidence of the end of prompt emission (Zhang et al. 2006). The nature of the X-ray emission detected at $t > 3 \times 10^4$ s is hard to pin down. Its spectrum is very soft (photon index $\Gamma = 3.3^{+2.2}_{-1.6}$), similar to that of XRF 060218. This is also unexpected in the external forward shock models, and this late X-ray component may be related to a late central engine afterglow, whose origin is unclear (e.g., Fan et al. 2006; Soderberg et al. 2006).

The prompt BAT/XRT data do not show a significant variability (Figure 2). The time-averaged γ-ray luminosity is $\sim 3 \times 10^{46}$ erg s^{-1} and the X-ray luminosity is $\sim 2 \times 10^{46}$ erg s^{-1}. The bolometric luminosity of the XRF outflow is therefore expected to be in the order of 10^{47} erg s^{-1}. The duration of the BAT emission is at least 1.23×10^3 s, and can be longer. The relatively steady energy output is naturally produced if *the central engine is a neutron star with significant dipole radiation*. The dipole radiation luminosity of a magnetized neutron star can be described as

$$L_{\rm dip} = 2.6 \times 10^{48}\ {\rm erg\ s^{-1}}\, B_{\rm p,14}^2 R_{\rm s,6}^6 \Omega_4^4 \left(1 + \frac{t}{\tau_0}\right)^{-2}, \quad (1)$$

where $B_{\rm p}$ is the dipole magnetic field strength of the neutron star at the magnetic pole, $R_{\rm s}$ is the radius of the neutron star, Ω is the angular frequency of radiation at $t = 0$, $\tau_0 = 1.6 \times 10^4 B_{\rm p,14}^{-2} \Omega_4^{-2} I_{45} R_{\rm s,6}^{-6}$ s is the corresponding spin-down timescale of the magnetar, and $I \sim 10^{45}$ g cm^2 is the typical moment of inertia of the magnetar (Pacini 1967; Gunn & Ostriker 1969). Here, the convention $Q_{\rm n} = Q/10^{\rm n}$ is adopted in cgs units. One then has $L_{\rm dip} \sim$ const for $t \ll \tau_0$ and $L_{\rm dip} \propto t^{-2}$ for $t \gg \tau_0$. An abrupt drop in the X-ray flux with a slope steeper than t^{-2} may be interpreted as a decrease of radiation efficiency, or the collapse of the neutron star into a black hole, possibly by losing the angular momentum or by accreting materials. Within such a model, the fact that

$$L_{\rm dip} \sim 10^{47}\ {\rm erg\ s^{-1}},\ \tau_0 \sim 1000\ {\rm s},$$

would require $(B_{\rm p,14}, \Omega_4, I_{45}, R_{\rm s,6}) \sim (30, 0.06, 1, 1)$. This is a slow ($P \simeq 10$ ms) magnetar ($B_{\rm p} \simeq 3 \times 10^{15}$ G).

The composition of this spin-down-powered outflow is likely Poynting-flux-dominated. Besides the magnetar argument (which naturally gives a highly magnetized outflow), another argument would be the lack of a bright thermal component with a temperature $kT \sim 10\ {\rm keV} L_{47}^{1/4} R_{0.9}^{-1/2}$ from the outflow photosphere as predicted in the baryonic outflow model, where R_0 is the initial radius where the outflow is accelerated (e.g., Zhang & Pe'er 2009; Fan 2010). One may argue that the photosphere radiation peaks at the observed $E_{\rm p}$. Such a scenario, however, is hard to account for the X-ray spectrum $F_\nu \propto \nu^{-0.32 \pm 0.03}$.

Below we discuss a possible magnetic dissipation scenario that would interpret XRF 100316D prompt emission. By comparing the pair density ($\propto r^{-2}$, r is the radial distance from the central source) and the density required for co-rotation ($\propto r^{-1}$ beyond the light cylinder of the compact object), one can estimate the radius at which the MHD condition breaks down, which reads $r_{\rm MHD} \sim 5 \times 10^{15} L_{47}^{1/2} \sigma_{1.6}^{-1} t_{v,m,-2} \Gamma_{\rm i,1.5}^{-1}$ cm, where σ is the ratio of the magnetic energy flux to the particle energy flux, $\Gamma_{\rm i}$ is the bulk Lorentz factor of the outflow, $t_{v,m} \sim P$ is the minimum variability timescale of the central engine (Zhang & Mészáros 2002; Fan et al. 2005; Gao & Fan 2006). Beyond this radius, intense electromagnetic waves are generated and outflowing particles are accelerated (Usov 1994; Lyutikov & Blackman 2001). Part of the Poynting flux energy is converted to radiation. At $r_{\rm MHD}$, the comoving magnetic fields $B_{\rm MHD}$ can be estimated as $B_{\rm MHD} \sim 20 \xi \sigma_{1.6} t_{v,m,-2}^{-1}$ G, where $\xi \leqslant 1$ reflects the efficiency of magnetic energy dissipation. When magnetic dissipation occurs, a fraction $\varepsilon_{\rm e}$ of the dissipated comoving magnetic energy would be eventually converted to the comoving kinetic energy of the electrons. Electrons may be linearly accelerated in the electric fields or stochastically accelerated in the random electromagnetic fields. One may assume that the accelerated electrons form a single power-law distribution in energy, i.e., $dn/d\gamma_{\rm e} \propto \gamma_{\rm e}^{-\rm p}$ for $\gamma_{\rm e} > \gamma_{\rm e,m}$, where $\gamma_{\rm e,m}$ can be estimated as $\gamma_{\rm e,m} \sim 3.5 \times 10^4 \sigma_{1.6} C_p$, and $C_p \equiv (\varepsilon_e/0.5)(p-2)/(p-1)$. At $r_{\rm MHD}$, the corresponding synchrotron radiation frequency is (Fan et al. 2005)

$$\nu_{\rm m,MHD} \sim 2 \times 10^{18}\ {\rm Hz}\, \xi \sigma_{1.6}^3 C_p^2 \Gamma_{\rm i,1.5} t_{v,m,-2}^{-1}. \quad (2)$$

The cooling Lorentz factor can be estimated by $\gamma_{\rm e,c} \sim 4.5 \times 10^{19} \Gamma_{\rm i}/(r_{\rm MHD} B_{\rm MHD}^2)$, which gives a synchrotron cooling frequency $\nu_{\rm c,MHD} \sim 6 \times 10^{14}\ {\rm Hz} \Gamma_{\rm i,1.5}^5 L_{47}^{-1} \xi^{-3} \sigma_{1.6}^{-1} t_{\rm v,m,-2}$. The observed XRT spectrum can be approximated by $F_\nu \propto \nu^{-0.3} - \nu^{-0.4}$, which is close to the fast cooling spectrum $\nu^{-1/2}$, suggesting $\nu_{\rm c,MHD} \lesssim 10^{17}$ Hz (it is straightforward to show that for the fiducial parameters adopted in this work the synchrotron self-absorption is below the optical band). On the other hand, the non-detection of prompt emission by UVOT (Starling et al. 2010) favors a high cooling frequency $\nu_{\rm c,MHD} \sim 2.4 \times 10^{17}$ Hz. As shown in Figure 4, the synchrotron radiation model with such a high $\nu_{\rm c,MHD}$ can roughly account for the data. We then get a constraint

$$\Gamma_{\rm i} \sim 60 L_{47}^{1/5} \xi_{-0.3}^{3/5} \sigma_{1.6}^{1/5} t_{\rm v,m,-2}^{-1/5} (\nu_{\rm c,MHD}/2.4 \times 10^{17}\ {\rm Hz})^{1/5}.$$

[6] With the simplest assumptions that (1) the opacity of the SN outflow is from Thompson scattering of electrons and is ~ 0.2 g^{-1} cm^2 and that (2) the density of expanding SN material takes the form $\propto R^{-k}$ ($k \sim 6$–8; J. S. Deng 2010, private communication, see also Matzner & McKee 1999; Berger et al. 2002; Chevalier & Fransson 2006), it is straightforward to show that the mass of the SN material moving faster than $V_{\rm s}$ is $M_{\rm SN}(>V_{\rm s}) \sim 8\pi \frac{k-1}{k-3} \frac{m_p}{\sigma_{\rm T}} V_{\rm s}^2 t^2$, where $V_{\rm s}$ is the photospheric velocity at t, $\sigma_{\rm T}$ is the Thompson scattering cross section, and $m_{\rm p}$ is the rest mass of proton. The corresponding kinetic energy is $E_{\rm k,SN}(>V_{\rm s}) \sim 4\pi \frac{k-1}{k-5} \frac{m_p}{\sigma_{\rm T}} V_{\rm s}^4 t^2$. For SN 2010bh, $V_{\rm s} \sim 0.09c$ at $t \sim 21$ days, we have $E_{\rm k,SN10bh}(>0.09c) \sim 1.6 \times 10^{52} [(k-1)/3(k-5)]$ erg.

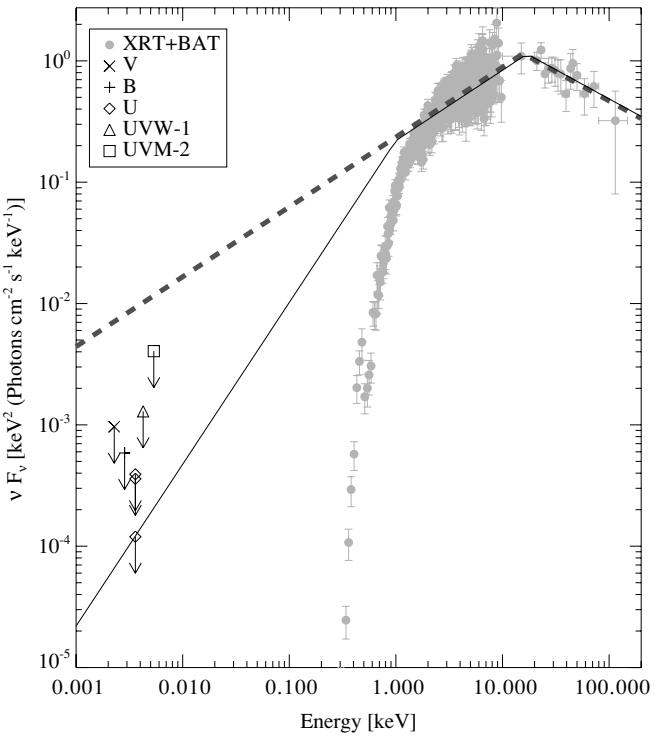

Figure 4. Broadband SED from UVOT, XRT, and BAT data. Gray points show the time-averaged BAT+XRT spectrum between $T_{\rm trig}$ + 150 s and $T_{\rm trig}$ + 744 s. The thick dashed line represents an absorbed broken power-law fit (i.e., wabs*zwabs*bknpower in XSPEC although the absorption components are not plotted here) to the BAT+XRT data leading to $\Gamma_1 = 1.42$, $\Gamma_2 = 2.48$ and $E_{\rm break} = 16$ keV. The solid line shows the same fitting as above for higher energy band but with an additional break at 1 keV, below which the photon index is set to $-2/3$. UVOT observations are taken from Starling et al. (2010). The extinction in each filter has been corrected by adopting $E_{\rm MW}(B-V) = 0.12$ from the Milky Way and $E_{\rm host}(B-V) = 0.1$ from the host galaxy (Starling et al. 2010; Chornock et al. 2010) and a Milky Way like extinction curve for all bands (Pei 1992).

Substituting this into Equation (2), we get

$$\sigma \sim 54 L_{47}^{-1/16} \left(\frac{\nu_{\rm c,MHD}}{2.4\times10^{17}\ {\rm Hz}}\right)^{-1/16} \xi_{-0.3}^{-1/2} C_{\rm p}^{-5/8} t_{\rm v,m,-2}^{3/8}.$$

Within such a scenario, $E_{\rm p}$ is defined by $\nu_{\rm m,MHD}$ (Equation (2)). An observed evolving $E_{\rm p}$ may be understood by invoking a decreasing σ, which is consistent with the magnetic field dissipation hypothesis. For $\nu > E_{\rm p}/h$ (where h is Planck's constant), the spectrum is $F_\nu \propto \nu^{-p/2}$.

The typical variability timescale of the radiation powered by the magnetic energy dissipation can be estimated as

$$\delta t \sim r_{\rm MHD}/\left(2\Gamma_{\rm i}^2 c\right) \sim 10\ {\rm s} L_{47}^{1/2} (\sigma/50)^{-1} t_{v,m,-2} (\Gamma_{\rm i}/60)^{-3}, \quad (3)$$

which is much larger than the rotation period $P \sim 10$ ms of the magnetar, implying that the pulsation of the central engine is undetectable.

4. DISCUSSION AND SPECULATIONS

So far the nearby supernova-associated GRBs, except GRB 030329, are found to be intrinsically underluminous. They share the similarities such as low isotropic energies and smooth light curves, but differ in some aspects. For example, GRB 980425 and GRB 031203 have shorter durations and higher $E_{\rm p}$'s than XRF 060218 and XRF 100316D. The underlying physical processes that result in these differences are not well understood. Through supernova modeling, it is found that GRB 980425 and GRB 031203 have a progenitor star massive enough to form a black hole (Deng et al. 2005; Mazzali et al. 2006a), while XRF 060218 has a less massive progenitor that most plausibly produces a neutron star (Mazzali et al. 2006b). The luminosity and the duration of XRF 100316D are consistent with the radiation from a neutron star with a dipole magnetic field $B_{\rm p} \sim 3\times10^{15}$ G and a rotation period $P \sim 10$ ms. This seems to point toward a hypothesis that two types of central engines define the apparent dichotomy of the SN-associated LL-GRBs, i.e., black hole engines give rise to "shorter" and "harder" GRBs such as GRB 980425 and GRB 031203, while magnetar engines give rise to very long and soft XRFs such as XRF 060218 and XRF 100316D.[7]

Adding in SN data makes the scenario more complicated. Although SN 2006aj associated with XRF 060218 does not conflict with a slow magnetar central engine, SN 2010bh associated with XRF 100316D may be too energetic to be interpreted with a slow magnetar central engine. If it is confirmed that the kinetic energy of SN 2010bh is in excess of 10^{52} erg, neither the neutrino energy nor the magnetar spin energy ($\sim10^{50}$ erg) is adequate to power the SN. A salient feature of the dipole spin-down formula (Equation (1)) is that if one shifts the time zero point (e.g., $t' = t - t_0$), the spin-down law still applies, with the initial angular frequency re-defined as $\Omega' = \Omega(t' = 0)$, and the characteristic spin-down timescale re-defined as $\tau_0' = 1.6\times10^4 B_{\rm p,14}^{-2}\Omega_4'^{-2} I_{45} R_{s,6}^{-6}$. This suggests that the observed plateau feature can be still interpreted if the initial period is much shorter than 10 ms, say, $P_0 \sim 1$ ms, if the time zero point is much earlier than $T_{\rm trig} - 500$ s (i.e., $t = 0$). This is because a power-law decay light curve may show an artificial plateau in the log–log space, if the zero time is misplaced to a later epoch (Yamazaki et al. 2009; Liang et al. 2009). Within such a scenario, a nascent magnetar was born with an initial period $P_0 \sim 1$ ms at $t \sim -5\times10^3$ s. Its initial dipole radiation was trapped by the envelope of the progenitor and could not escape. This spin-down energy gives enough impetus to explode the star and power the energetic SN 2010bh. After a significant delay ($\sim5\times10^3$ s to spin down from 1 ms to 10 ms for $B_{\rm p} \sim 3\times10^{15}$ G), the magnetar wind finally managed to escape as a relativistic Poynting-flux-dominated outflow. An observer noticed the jet emission only around $t = 0$. The above argument also applies to the model of fallback accretion onto a nascent black hole.

With such a hypothesis, one may envision a unified picture to understand the diversity of GRB/SN associations by invoking a variety of initial powers and the delay times between the core collapse and the emergence of the relativistic jet from the star. The speculation is the following.

1. To produce an energetic SN/luminous GRB (e.g., GRB 030329/SN 2003dh), the central engine is powerful (a black hole with an accretion disk or a rapidly spinning magnetar) and the relativistic outflow can break out the progenitor soon enough when the engine is still working effectively.
2. To produce an energetic SN/underluminous GRB (e.g., GRB 980425/SN 1998bw, GRB 031203/SN 2003lw, and

[7] We caution that such a scenario is not robust, since a magnetar engine may also drive SN 1998bw (Woosley 2010), and a black hole engine may be also able to reproduce the XRF 100316D-like light curves through tuning the parameters of fall-back materials and arguing for a Poynting-flux-dominated outflow from a highly magnetized black hole engine (e.g., MacFadyen et al. 2001; Zhang et al. 2008).

XRF 100316D/SN 2010bh), the central engine is initially powerful, but it takes time for the relativistic wind to emerge from the star. As it breaks out the star, the central engine already fades down with a decreased power. The longer, softer XRFs are probably powered by a magnetar, while the shorter, harder GRBs are probably powered by a black hole.

3. To produce a less-energetic SN/underluminous GRB (e.g., XRF 060218/SN 2006aj), the central engine is a slow magnetar with an initial rotation energy less than 10^{51} erg. The emergence of the relativistic outflow can be prompt or somewhat (but not significantly) delayed.

Finally, a straightforward expectation from the speculation that XRF 100316D outflow is Poynting-flux-dominated is that the prompt emission should be linearly polarized (e.g., Fan et al. 2005). The polarimetry measurements of events such as XRF 100316D and XRF 060218 would provide a criterion to differentiate this model from the shock breakout model, which does not predict a strong polarization signal.

We thank the anonymous referee for helpful comments, and S. Covino, J. S. Deng, and R. L. C. Starling for communications. This work was supported in part by the National basic research program of China under grant 2009CB824800 (for Y.Z.F. and E.W.L), and by NASA NNX09AT66G, NNX10AD48G, and NSF AST-0908362 (for B.Z.).

REFERENCES

Berger, E., Kulkarni, S. R., & Chevalier, R. A. 2002, ApJ, 577, L5
Campana, S., et al. 2006, Nature, 442, 1008
Chevalier, R. A., & Fransson, C. 2006, ApJ, 651, 381
Chornock, R., et al. 2010, arXiv:1004.2262
Coward, D. M. 2005, MNRAS, 360, L77
Deng, J. S., et al. 2005, ApJ, 624, 898
Fan, Y. Z. 2010, MNRAS, 403, 483
Fan, Y. Z., Piran, T., & Xu, D. 2006, J. Cosmol. Astropart. Phys., JCAP09(2006)013
Fan, Y. Z., Zhang, B., & Proga, D. 2005, ApJ, 635, L129
Galama, T. J., et al. 1998, Nature, 395, 670
Gao, W. H., & Fan, Y. Z. 2006, Chin. J. Astron. Astrophys., 6, 513
Gehrels, N., et al. 2004, ApJ, 611, 1005
Guetta, D., & Della Valle, M. 2007, ApJ, 657, L73
Gunn, J., & Ostriker, J. 1969, Nature, 221, 454
Hjorth, J., et al. 2003, Nature, 423, 847
Li, L. X. 2006, MNRAS, 372, 1357
Liang, E., Zhang, B., Virgili, F., & Dai, Z. G. 2007a, ApJ, 662, 1111
Liang, E. W., Zhang, B. B., & Zhang, B. 2007b, ApJ, 670, 565
Liang, E.-W., et al. 2009, ApJ, 707, 328
Lyutikov, M., & Blackman, E. G. 2001, MNRAS, 321, 177
MacFadyen, A. I., Woosley, S. E., & Heger, A. 2001, ApJ, 550, 410
Malesani, D., et al. 2004, ApJ, 609, L5
Matzner, C. D., & McKee, C. F. 1999, ApJ, 510, 379
Mazzali, P. A., et al. 2006a, ApJ, 645, 1323
Mazzali, P. A., et al. 2006b, Nature, 442, 1018
Pacini, F. 1967, Nature, 216, 567
Pei, Y. C. 1992, ApJ, 395, 130
Rau, A., et al. 2010, GCN Circ., 10547
Soderberg, A., et al. 2006, Nature, 442, 1014
Stamatikos, M., et al. 2010, GCN Circ., 10496
Starling, R. L. C., et al. 2010, MNRAS, submitted (arXiv:1004.2919)
Toma, K., Ioka, K., Sakamoto, T., & Nakamura, T. 2007, ApJ, 659, 1420
Usov, V. V. 1994, MNRAS, 267, 1035
Vergani, S. D., et al. 2010, GCN Circ., 10512
Wiersema, K., et al. 2010, GCN Circ., 10525
Woosley, S. E. 2010, ApJ, 719, L204
Yamazaki, R., et al. 2009, ApJ, 690, L118
Zhang, B., & Mészáros, P. 2002, ApJ, 566, 712
Zhang, B., & Pe'er, A. 2009, ApJ, 700, L65
Zhang, B., et al. 2006, ApJ, 642, 354
Zhang, B. B., Liang, E. W., & Zhang, B. 2007, ApJ, 666, 1002
Zhang, W. Q., Woosley, S. E., & Heger, A. 2008, ApJ, 679, 639